CHAPTER 5: Lithography

Lithography is the process of transferring patterns of geometric shapes in a mask to a thin layer of radiation-sensitive material (called resist) covering the surface of a semiconductor wafer. ***Figure 5.1*** illustrates schematically the lithographic process employed in IC fabrication. As shown in ***Figure 5.1(b)***, the radiation is transmitted through the clear parts of the mask and makes the exposed photoresist insoluble in the developer solution, thereby enabling the direct transfer of the mask pattern onto the wafer. After the patterns are defined, an etching process is employed to selectively remove masked portions of the underlying layer.

The performance of a lithographic exposure is determined by three parameters: resolution, registration, and throughput. Resolution is defined to be the minimum feature dimension that can be transferred with high fidelity to a resist film on a semiconductor wafer. Registration is a measure of how accurately patterns on successive masks can be aligned or overlaid with respect to previously defined patterns on the same wafer. Throughput is the number of wafers that can be exposed per hour for a given mask level and is thus a measure of the efficiency of the lithographic process.

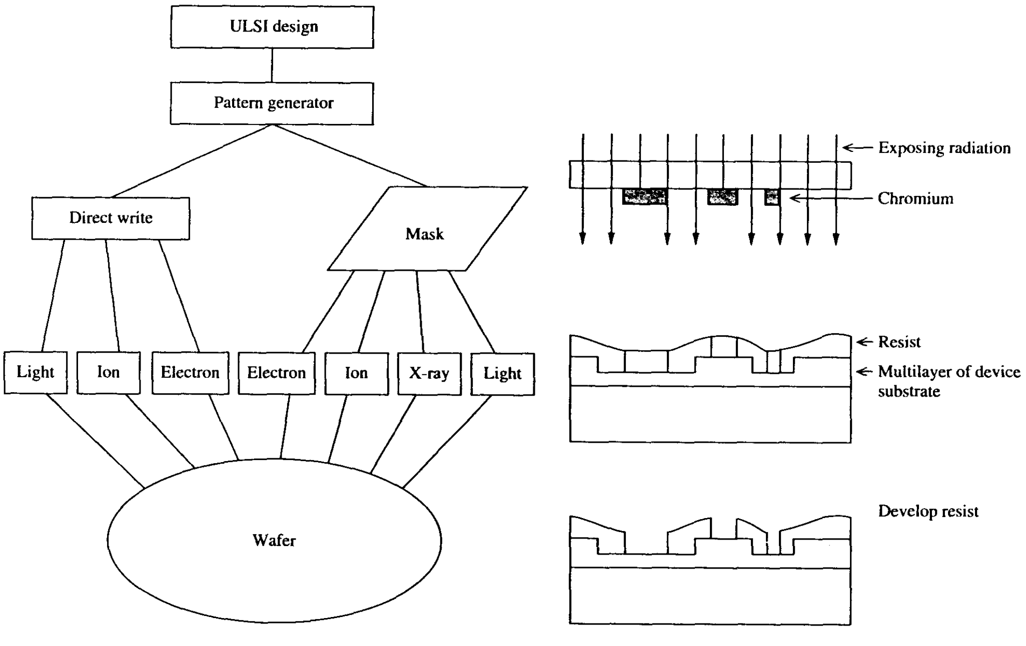

(*a*) (*b*)

Figure 5.1: (**a**) Lithographic process flow chart. (**b**) Optical replication process.

5.1 Clean Room

An IC fabrication facility requires a clean room, particularly in lithography areas. Dust particles settling on semiconductor wafers and lithographic masks can cause defects in the devices. As illustrated in ***Figure 5.2***, airborne particles adhering to the surface of a photomask behave as opaque patterns that can be subsequently transferred to the circuit patterns, thus leading to deleterious ramifications. For example, particle 1 in ***Figure 5.2*** may result in the formation of a pinhole in the underlying layer. Particle 2 may cause a constriction of current flow in the metal runner, whereas particle 3 may lead to a short circuit between the two conducting regions and render the circuit useless.

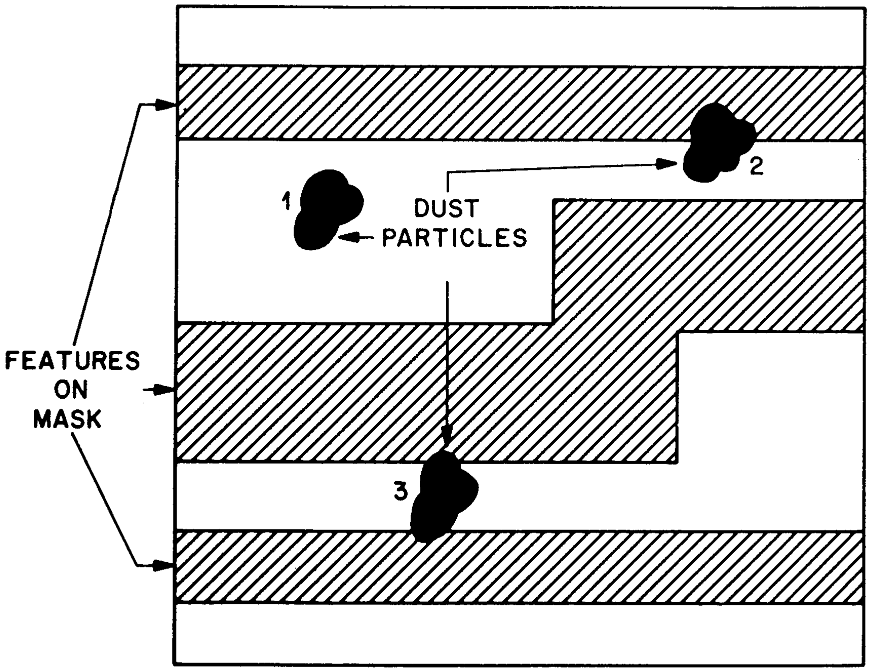

Figure 5.2: Various ways in which dust particles can interfere with photomask patterns.

In a clean room, the total number of dust particles per unit volume must be tightly controlled along with other parameters such as temperature, humidity, pressure, and so on. A class *X* clean room is usually defined to be one that has a dust count of *X* particles (diameters of 0.5 μm or larger) per cubic foot. As shown in ***Figure 5.3***, the particle count is higher as the particle size becomes smaller. For modern lithographic processes, a class 10 or better clean room is required.

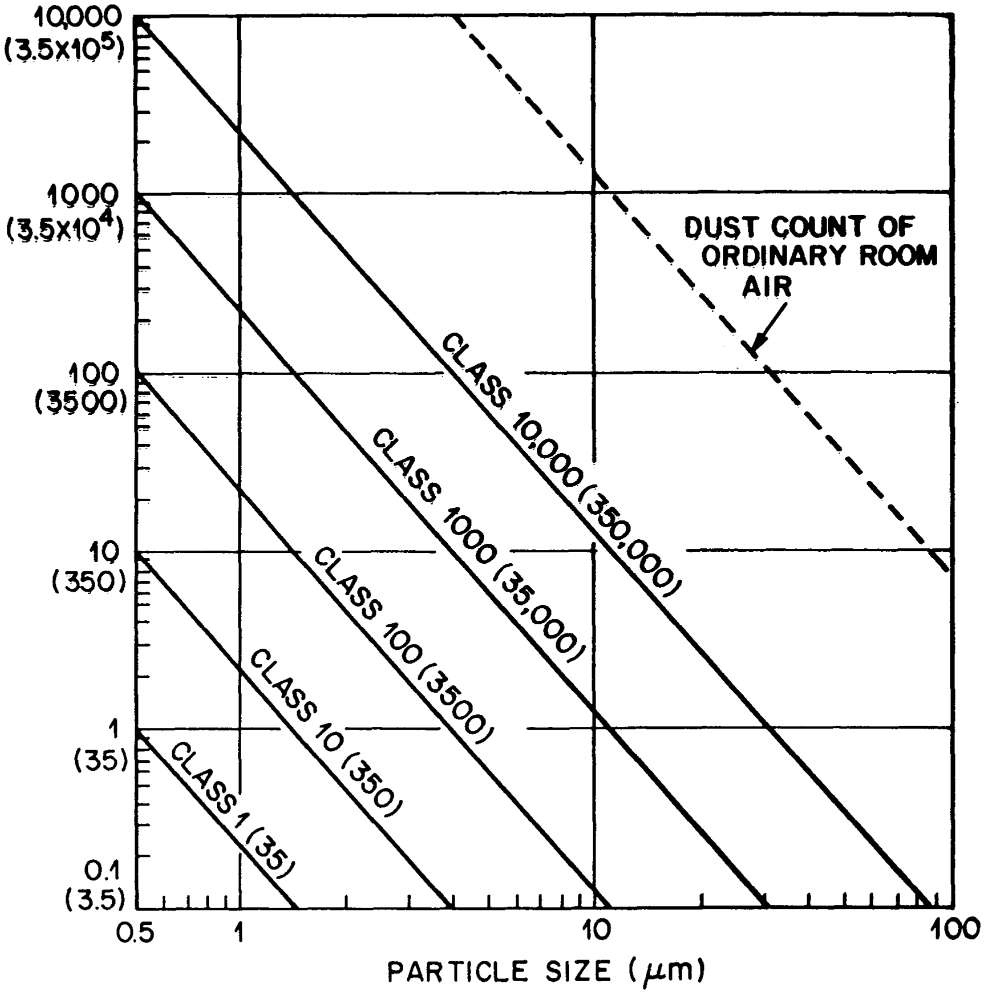

***Figure* 5.3**: Particle-size distribution curve.

For more detailed discussions on cleanroom technology and design, please peruse Chapter 1 of ULSI Technology.

Example 5.1

If a 125-mm diameter wafer is exposed to for 1 minute to an air stream under a laminar-flow condition at 30 m/min, how many dust particles will land on the wafer in a class 10 clean room?

Solution

For a class 10 clean room, there are 350 particles (0.5 µm or larger) per cubic meter. The air volume that goes over the wafer in 1 min is:

$$(30\ \text{m/min})\ \text{x}\ \pi \left[\frac{0.125m}{2}\right]^2\ \text{x}\ 1\ \text{min} = 0.368\ \text{m}^3$$

The number of dust particles (0.5 µm or larger) contained in the air volume is

$$350\ \text{x}\ 0.368 = 128\ \text{particles}$$

Therefore, if there are 200 IC chips on the wafer, the particle count amounts to one particle on each of 64% of the chips. Fortunately, only a fraction of the particles that land adhere to the wafer surface, and of those only a fraction are at a circuit location critical enough to cause a failure. However, the calculation indicates the importance of the clean room.

5.2 Optical Lithography

The vast majority of lithographic equipment for IC fabrication is optical equipment using ultraviolet light ($\lambda \cong 0.2$ µm to 0.4 µm) or deep ultraviolet light. There are basically two optical exposure methods: shadow printing and projection printing.

In shadow printing, the mask and wafer may be in direct contact, as in contact printing, or in close proximity, as in proximity printing (***Figure 5.4***). Contact printing yields very high resolution (~ 1 µm), but suffers from major drawback caused by dust particles or silicon specks accidentally embedded into the mask, thereby causing permanent damage to the mask and defects in the wafers. Proximity printing is not as prone to particle damage. However, the small gap between the mask and wafer (typically 10 µm to 50 µm) introduces optical diffraction at the feature edges on the photomasks and the resolution is typically degraded to the 2 to 5 µm regime.

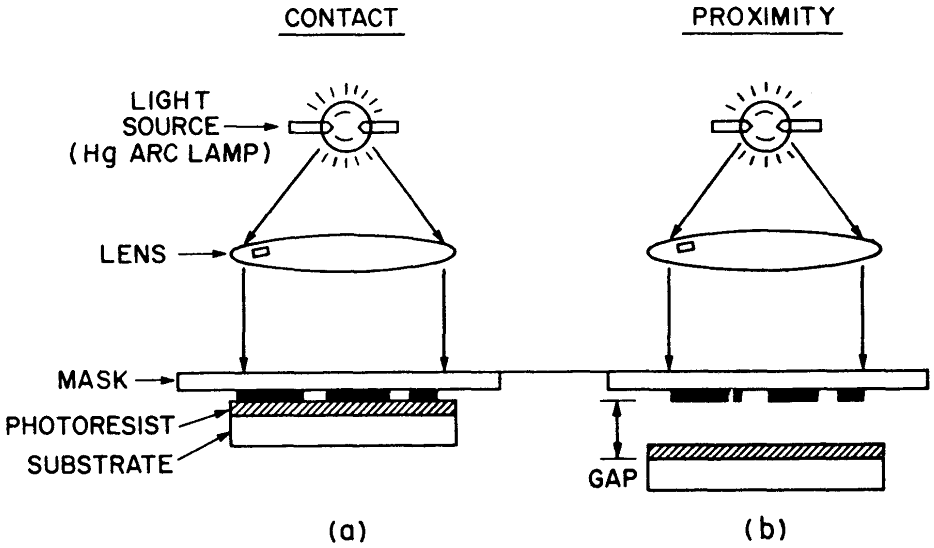

Figure 5.4: (**a**) Contact printing. (**b**) Proximity printing.

The minimum line-width that can be printed, l_m, in shadow printing is roughly given by:

$$l_m = (\lambda g)^{1/2} \qquad \textit{(Equation 5.1)}$$

where λ is the wavelength of the exposure radiation and g is the gap between the mask and the wafer and includes the thickness of the resist. For typical values of λ (~ 0.4 μm) and g (~ 50 μm), l_m is on the order of 4.5 μm. *Equation 5.1* imparts that the minimum linewidth can be improved by reducing the wavelength λ (that is, going to deep UV spectral region) or the gap g.

In order to circumvent problems associated with shadow printing, projection printing exposure tools have been developed to project an image of the mask patterns onto a resist-coated wafer many centimeters away from the mask. The small image area is scanned or stepped over the wafer to cover the entire surface. ***Figure 5.5*** depicts the various ways to project and scan the image. The resolution of a projection system is given by:

$$l_m = \lambda / NA \qquad \textit{(Equation 5.2)}$$

where λ is the wavelength of the exposure radiation and NA is the numerical aperture given by:

$$NA = \bar{n}\sin\theta \qquad \textit{(Equation 5.3)}$$

where $\bar{n}$ denotes the refraction index of the imaging medium ($\bar{n}$ = 1 in air) and θ is the half angle of the cone of light converging to a point image at the wafer as shown in ***Figure 5.6***. The depth of focus, Δz, can be expressed as:

$$\Delta z = \pm l_m/2\tan\theta \cong \pm l_m/2\sin\theta = \pm \bar{n}\lambda/[2(NA)^2] \qquad \textit{(Equation 5.4)}$$

Resolution can be enhanced by reducing λ and this explains the trend towards shorter wavelength in optical lithography. Typically, scanning projection systems are capable of about 1 μm resolution, while step-and-repeat projection systems can accomplish deep sub-micrometer spatial resolution demanded by modern integrated circuits, especially when coupled with deep UV radiation sources.

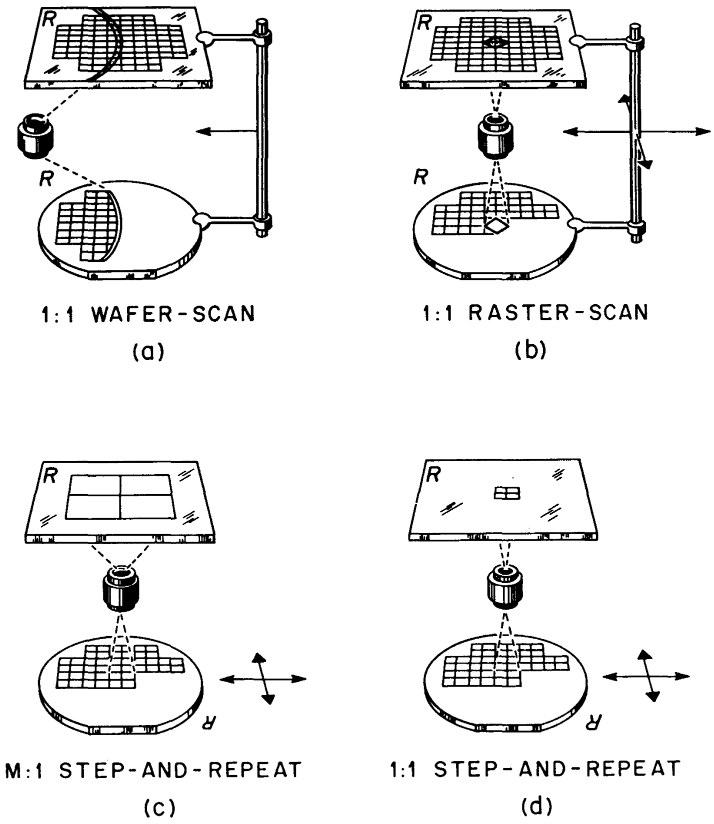

Figure 5.5: Image transfer techniques for projection printing. (**a**) Annular-field wafer scan. (**b**) Small-field raster scan. (**c**) Reduction step-and-repeat. (**d**) 1:1 step and repeat.

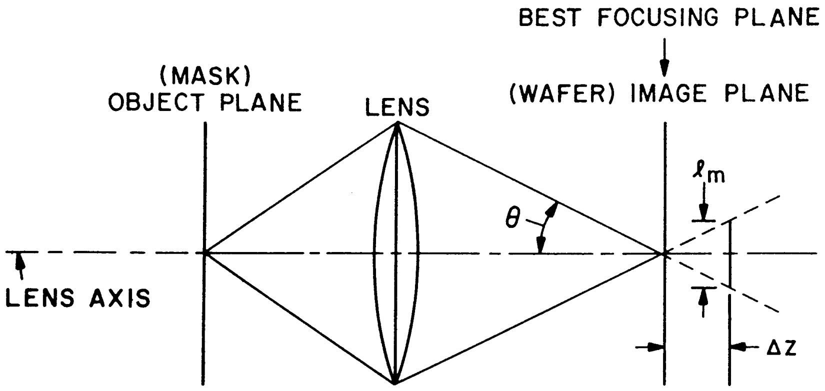

Figure 5.6: Simple image system.

5.3 Masks

For VLSI (> 10^5 components/chip) and ULSI (> 10^7 components / chip), the patterns are generated using computer-aided design (CAD) systems. The digital CAD output drives a pattern generator that transfers the patterns directly to the photosensitive masks. Masks are typically made from glass covered with hard-surface materials such as chromium or iron oxide. The number of mask defects has a profound effect on the final IC yield, which is defined as the ratio of good chips per wafer to the total number of chips per wafer. As a first-order approximation,

$$Y \cong \exp\{-DA\} \qquad \textit{(Equation 5.5)}$$

where Y is the yield, D is the average number of "fatal" defects per unit area, and A is the area of an IC chip. If D remains the same for all mask levels, N, then

$$Y \cong \exp\{-NDA\} \qquad \textit{(Equation 5.6)}$$

Figure 5.7 shows the mask-limited yield for a 10-level lithographic process as a function of chip size for various values of defect densities.

A phase-shifting mask is employed to reduce the problems arising from wavelength or depth of focus (DOF). The basic concept of the phase-shifting mask is illustrated in ***Figure 5.8***. At the conventional transmission mask (***Figure 5.8a***), the electric field ξ has the same phase at every aperture (clear area). Diffraction and the limited resolution of the optical system spread the electric field ξ at the wafer, as shown by the dotted line. Interference between waves diffracted by the adjacent apertures enhances the field between them. The intensity I is proportional to the square of the electric field.

The phase-shifting layer that covers adjacent apertures reverses the sign of the electric field as shown in ***Figure 5.8(b)***. The intensity at the mask is unchanged. However, the electric field of these images at the wafer, shown by the dotted line, can be canceled. Consequently, images that are projected close to one another can be separated completely. A 180° phase change occurs when a transparent layer of thickness $d = \lambda / 2(n - 1)$, where n is the refraction index and λ is the wavelength, covers one aperture as shown in ***Figure 5.8(b)***.

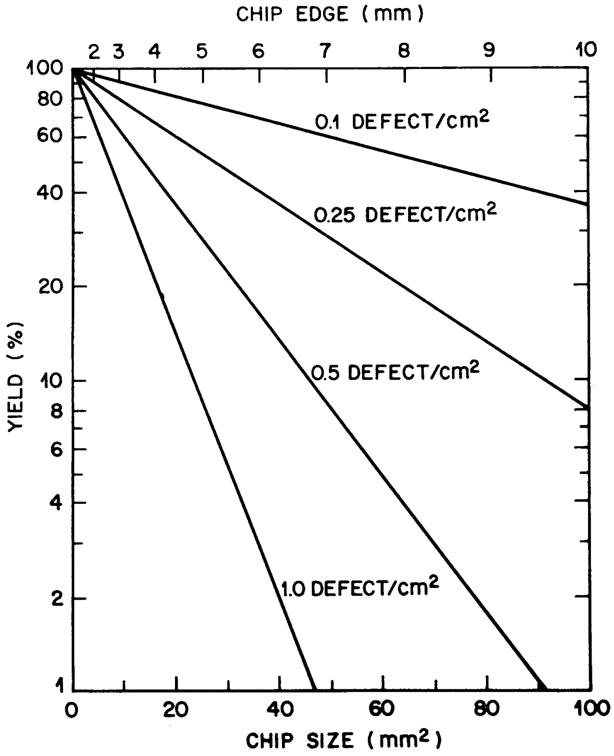

Figure 5.7: Yield for a 10-mask lithographic process with various defect densities per level.

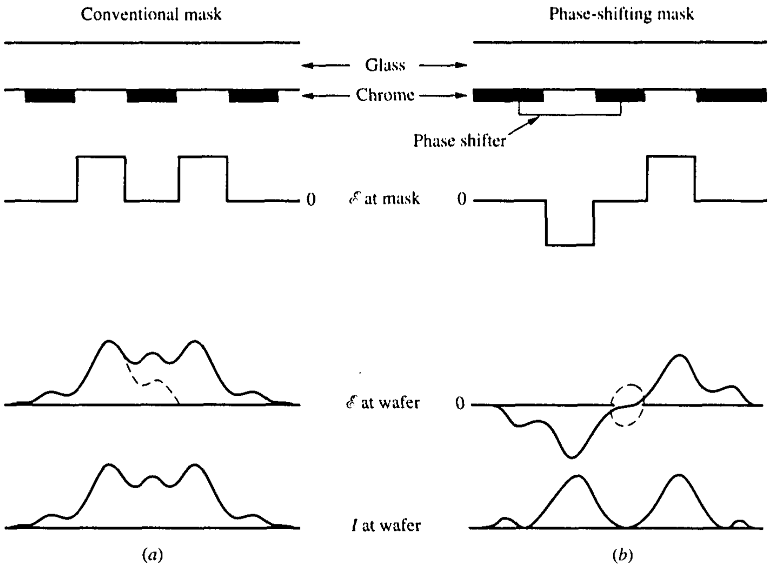

Figure 5.8: The principle of phase-shift technology. (**a**) Conventional technology. (**b**) Phase-shifting technology.

Example 5.2

The killing defect density is responsible for yield loss and depends on the design rule or size of the device on a chip. This is because when the design rule becomes smaller, a smaller particle can contribute to yield loss. For a 16M DRAM chip, the design rule is 0.5 µm, chip size is 1.4 cm^2, and killing defect size is 0.18 µm. Due to contamination that occurs in a cleanroom, the wafer defect density measured at size 0.3 µm increases fivefold from 0.2 D/cm^2 to 1.0 D/cm^2. Using the relationship $Y = e^{-DA}$ where D is the defect density and A is the chip area, calculate the yield loss of a 16M DRAM wafer due to the increase in the aforementioned defect density assuming that the defect density is roughly inversely proportional to the defect size to the second power.

Solution

The defect density is inversely proportional to the defect size. That is, the killing defect density $D = 0.2 \times (0.3/0.18)^2 = 0.2 \times 2.78 = 0.56$.

The yield before contamination is $Y = e^{-(0.56)(1.4)} = 0.45.7$ or 45.7%

Due to contamination, $D = 1 \times (0.3/0.18)^2 = 2.78$

The yield after contamination is $Y = e^{-(2.78)(1.4)} = 0.02$ or 2%.

5.4 Photoresist

A photoresist is a radiation-sensitive compound. For positive resists, the exposed region becomes more soluble and thus more readily removed in the developing process. The net result is that the patterns formed in the positive resist are the same as those on the mask. For negative resists, the exposed regions become less soluble, and the patterns engraved are the reverse of the mask patterns.

A positive photoresist consists of three constituents: a photosensitive compound, a base resin, and an organic solvent. Prior to exposure, the photosensitive compound is insoluble in the developer solution. After irradiation, the photosensitive compound in the exposed pattern areas absorbs energy, changes its chemical structure, and transforms into a more soluble species. Upon developing, the exposed areas are expunged.

Negative photoresists are polymers combined with a photosensitive compound. Following exposure, the photosensitive compound absorbs the radiation energy and converts it into chemical energy to initiate a chain reaction, thereby causing crosslinking of the polymer molecules. The cross-linked polymer has a higher molecular weight and becomes insoluble in the developer solution. After development, the unexposed portions are removed. One major drawback of a negative photoresist is that the resist absorbs developer solvent and swells, thus limiting the resolution of a negative photoresist.

Figure 5.9a exhibits a typical exposure response curve for a positive resist. Note that the resist has a finite solubility in the developer solution even prior to exposure. At a threshold energy, E_T, the resist becomes completely soluble. E_T therefore corresponds to the sensitivity of the photoresist. Another parameter, γ, is the contrast ratio and is given by:

$$\gamma = \left[\ln \frac{E_T}{E_1}\right]^{-1} \qquad \textit{(Equation 5.7)}$$

A larger γ implies a more rapid dissolution of the resist with an incremental increase of exposure energy and results in a sharper image. The image cross section depicted in ***Figure 5.9a*** illustrates that the edges of the resist image are generally blurred due to diffraction.

Figure 5.9b shows an analogous situation but for a negative photoresist. The sensitivity of a negative photoresist is defined as the energy required to retain

50% of the original resist film thickness in the exposed region. ***Table 5.1*** lists some of the resists commonly used in VLSI.

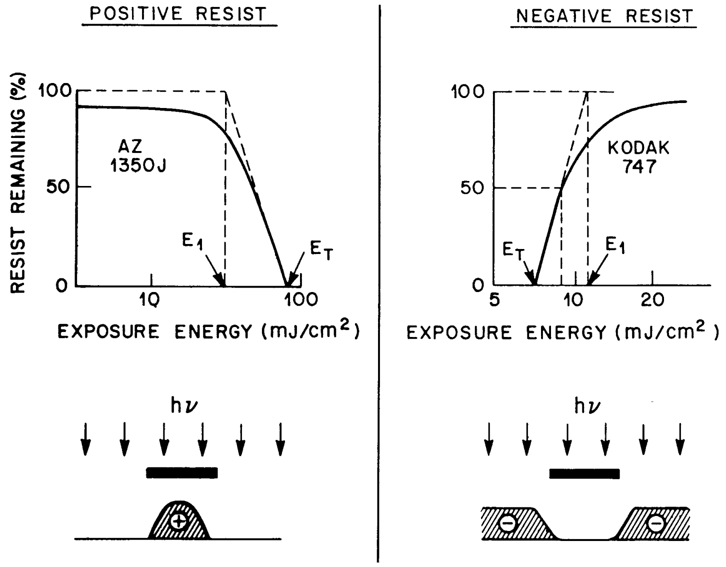

Figure 5.9: Exposure response curve and cross section of the resist image after development for positive photoresist (**left**) and negative photoresist (**right**).

Table 5.1: Negative and Positive Resists.

Lithography	Name	Type	Sensitivity	γ
Optical	Kodak 747	Negative	9 mJ/cm^2	1.9
	AZ-1350J	Positive	90 mJ/cm^2	1.4
	PR102	Positive	140 mJ/cm^2	1.9
e-beam	COP	Negative	0.3 μC/cm^2	0.45
	GeSe	Negative	80 μC/cm^2	3.5
	PBS	Positive	1 μC/cm^2	0.35
	PMMA	Positive	50 μC/cm^2	1.0
X-ray	COP	Negative	175 mJ/cm^2	0.45
	DCOPA	Negative	10 mJ/cm^2	0.65
	PBS	Positive	95 mJ/cm^2	0.5
	PMMA	Positive	1000 mJ/cm^2	1.0

5.5 Pattern Transfer

Figure 5.10 illustrates the steps of transferring IC patterns from a mask to a wafer. The wafer is placed in a clean room that typically is illuminated with yellow light as photoresists are not sensitive to wavelengths greater than 0.5 µm. The wafer is held on a vacuum spindle, and approximately 1 cm^3 of liquid resist is applied to the center of the wafer. The wafer is than spun for about 30 seconds. The thickness of the resulting resist film, l_R, is directly proportional to its viscosity as well as the percent solid content indigenous to the resist, and varies inversely with the spin speed. For spin speeds in the range of 1000 to 10000 rpm, film thicknesses on the order of 0.5 to 1 µm can be accomplished.

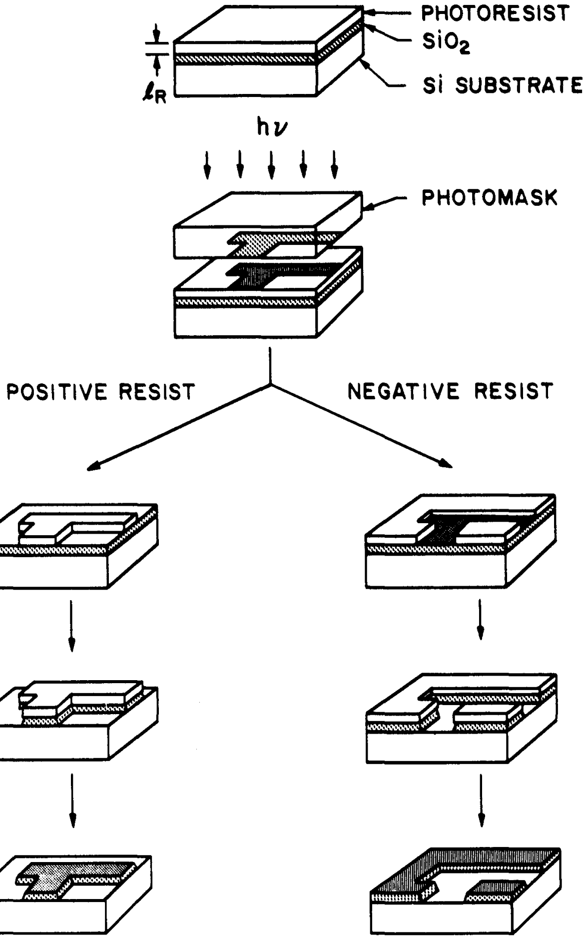

Figure 5.10: Optical lithographic transfer process.

The wafer is then given a pre-exposure bake (80°C to 100°C) to remove solvent and improve adhesion. The wafer is aligned with respect to the mask in an optical lithographic system prior to exposure to UV or deep UV light. For a positive photoresist, the exposed portions are dissolved in the developer solution. The wafer is then rinsed, dried, and then put in an ambient that etches the exposed insulating layer but does not attack the resist. Finally, the resist is stripped, leaving behind an insulator image (or pattern) that is the same as the opaque image on the mask. For a negative photoresist, the exposed area becomes insoluble, and the final insulator pattern is the reverse of the opaque image on the mask.

The insulator image can be employed as a mask for subsequent processing. For instance, ion implantation can be performed to dope the exposed regions selectively. ***Figure 5.11*** illustrates the lift-off technique. This method suffices if the film thickness is smaller than that of the photoresist.

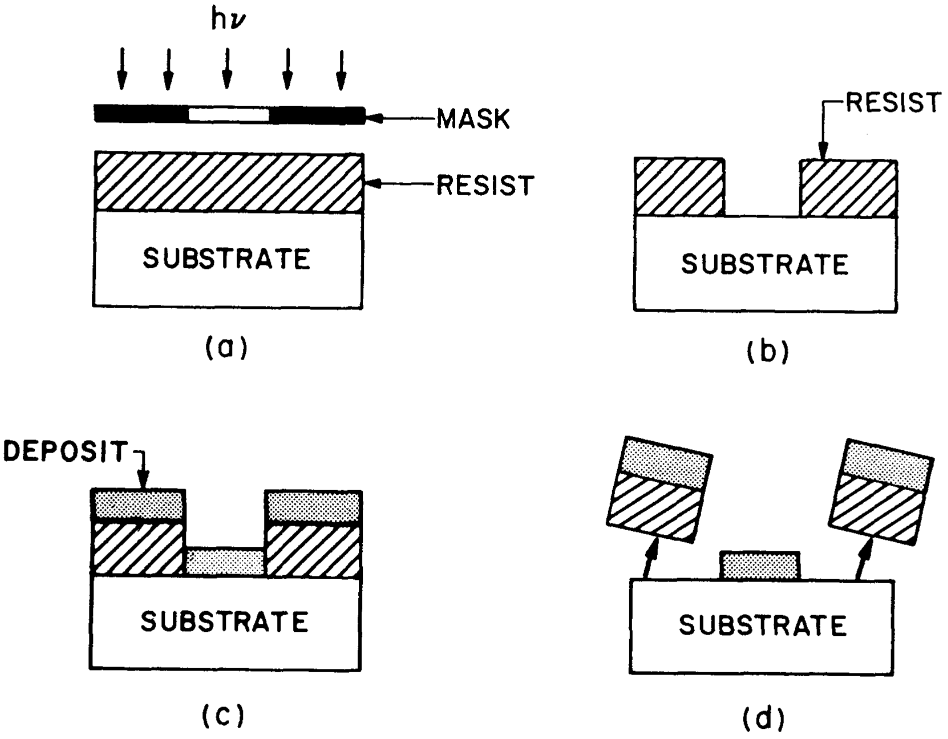

Figure 5.11: Lift-off process for pattern transfer.

5.6 Electron Lithography

Although optical lithography is most common, there exist other lithographic techniques, as depicted in ***Figure 5.12***. Electron lithography offers high resolution because of the small wavelength of electrons ($\leq$ 0.1 nm for 10-50 keV electrons). The resolution of an electron lithographic system is not limited by diffraction, but rather by electron scattering in the resist (***Figure 5.13***) and by the various aberrations of the electron optics. The advantages of electron lithography are:

(1) Generation of micron and submicron resist geometries

(2) Highly automated and precisely controlled operation

(3) Greater depth of focus

(4) Direct patterning without a mask

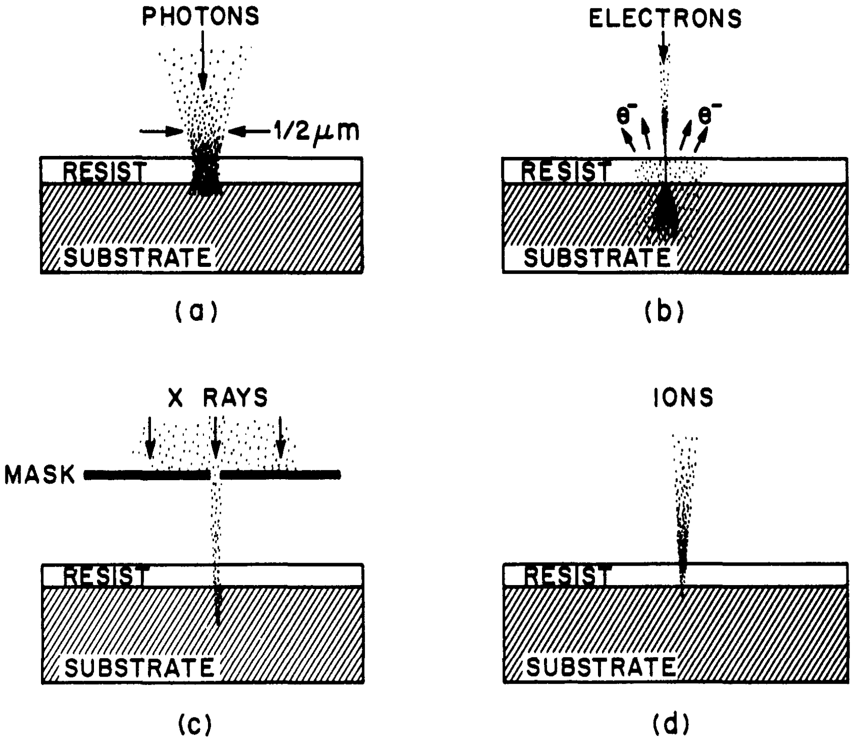

Figure 5.12: Types of lithographic methods. (**a**) Optical lithography. (**b**) Electron lithography. (**c**) X-ray lithography. (**d**) Ion lithography.

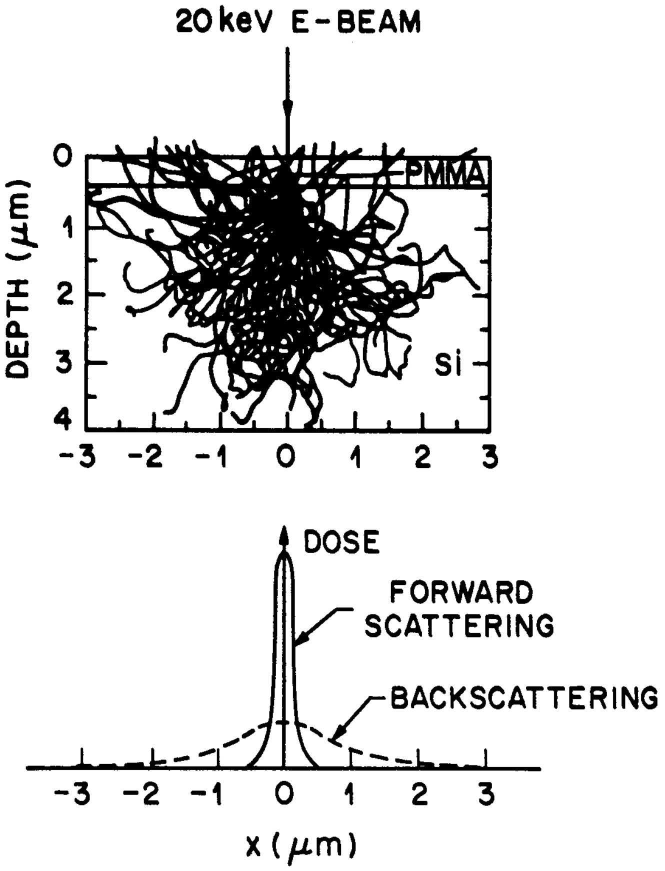

Figure 5.13: (**Top**) Simulated trajectories of 100 electrons in PMMA for a 20-keV electron beam. (**Bottom**) Dose distribution for forward scattering and backscattering at the resist – substrate interface.

The biggest disadvantage of electron lithography is its low throughput (approximately 5 wafers / hour at less than 0.1 μm resolution). Therefore, electron lithography is primarily used in the production of photomasks and in situations that require small number of custom circuits.

There are two basic ways to scan an electron beam. In raster scanning, the patterns are written by an electron beam that moves through a regular pattern. The beam scans sequentially over the entire area and is blanked off where no exposure is required. On the contrary, in vector scanning, the electron beam is directed only to the requested pattern features and hops from features to features. Time is therefore saved in a vector scan system.

Electron resists are polymers. For a positive electron resist, the polymer-electron interaction causes chain scission, that is, broken chemical bonds (***Figure 5.14 - top***). The irradiated areas can be dissolved in a developer solution that attacks low-molecular-weight material. Common positive electron resists are poly(methyl methacrylate), abbreviated PMMA, and poly(butene-1 sulfone), abbreviated PBS. Positive electron resists typically have resolution of 0.1 µm or better. When electrons impact a negative electron resist, polymer linking is induced (***Figure 5.14 - bottom***). Poly(glycidyl methacrylate-co-ethyl-acrylate), abbreviated COP, is a common negative electron resist. Like a negative photoresist, COP swells during developing, and resolution is limited to about 1 µm.

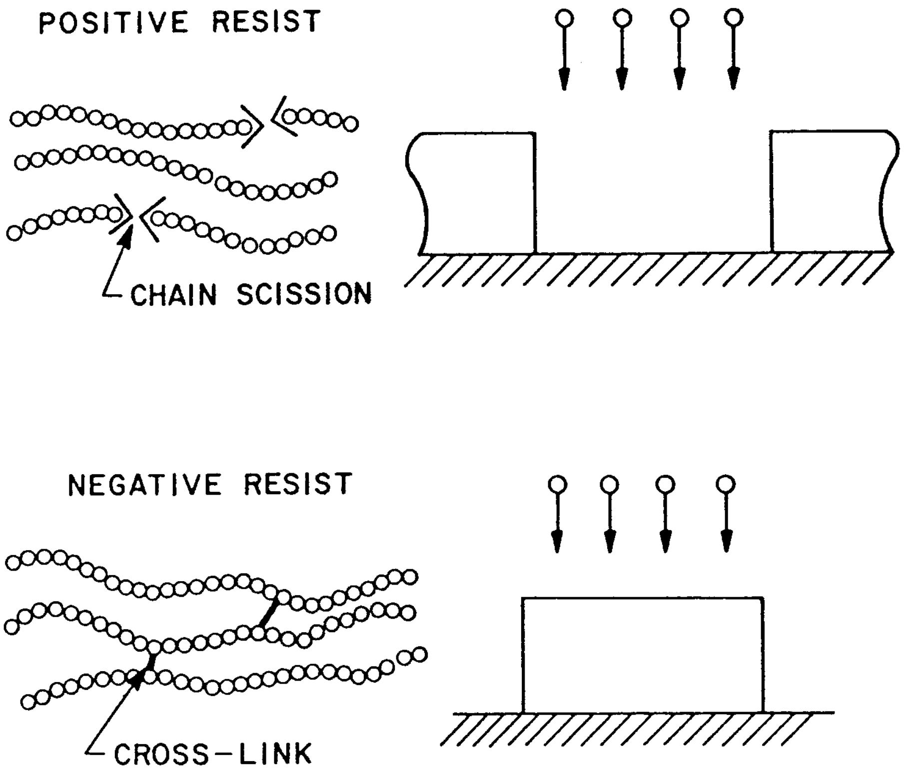

Figure 5.14: Schematic of the chemical reaction of a positive resist (**top**) and negative resist (**bottom**) used in electron beam lithography.

5.7 X-Ray Lithography

X-ray lithography employs a shadow printing method similar to optical proximity printing. The x-ray wavelength (0.4 to 5 nm) is much shorter than that of UV light (200 to 400 nm). Hence, diffraction effects are reduced and higher resolution can be attained. For instance, for an x-ray wavelength of 0.5 nm and a gap of 40 μm, l_m is equal to 0.2 μm. X-ray lithography has a higher throughput when compared to e-beam lithography because parallel exposure can be adopted. However, on account of the finite size of the x-ray source and the finite mask-to-wafer gap, a penumbral effect results which degrades the resolution at the edge of a feature. As shown in ***Figure 5.15***, the penumbral blur, δ, on the edge of the resist image is given by:

$$\delta = ag / L \qquad \textit{(Equation 5.8)}$$

where a is the diameter of the x-ray source, g is the gap spacing, and L is the distance from the source to the x-ray mask. If a = 3 mm, g = 40 μm, and L = 50 cm, δ is on the order of 0.2 μm.

An additional geometric effect is the lateral magnification error due to the finite mask-to-wafer gap and the non-vertical incidence of the x-ray beam. The projected images of the mask are shifted laterally by an amount d, called runout:

$$d = rg / L \qquad \textit{(Equation 5.9)}$$

where r denotes the radial distance from the center of the wafer. For a 125-mm wafer, the runout error can be as large as 5 μm for g = 40 μm and L = 50 cm. This runout error must be compensated for during the mask making process.

Electron beam resists can be used in x-ray lithography because when an x-ray photon impinges on the specimen, electron emission results. One of the most attractive x-ray resist is DCOPA (dichloropropyl acrylate and glycidyl methacrylate-co-ethyl acrylate), as it has a relatively low threshold (~ 10 mJ/cm^2).

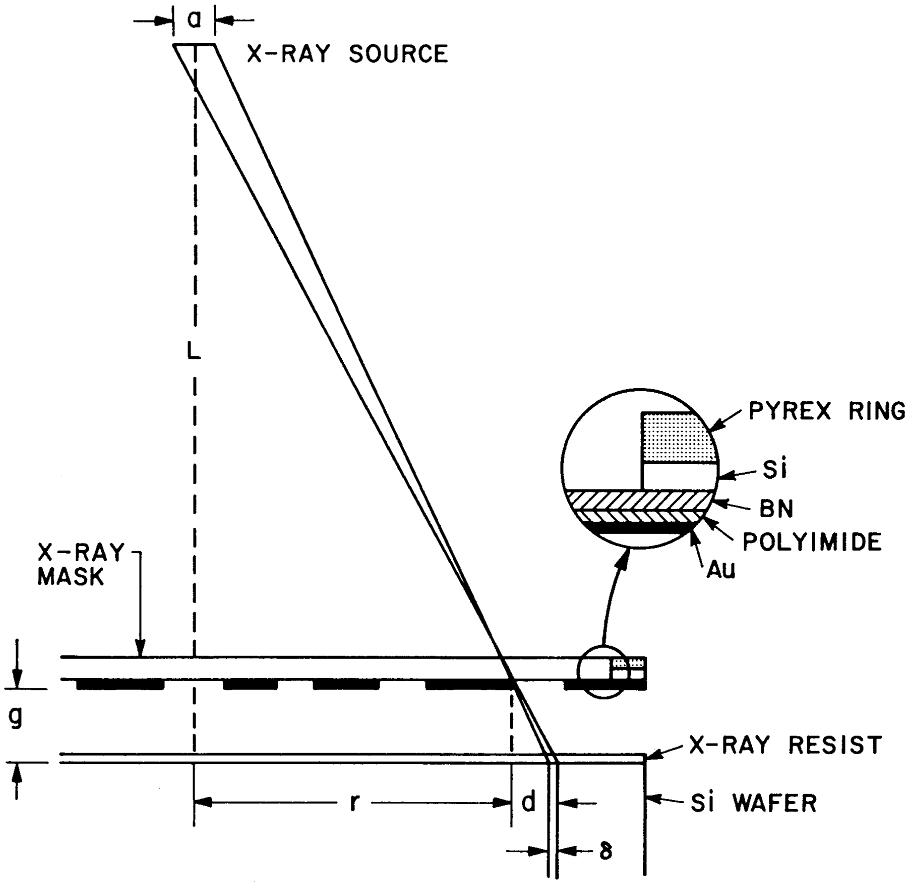

Figure 5.15: Geometric effects in x-ray lithography. Insert shows the x-ray mask structure.

5.8 Ion Lithography

Ion lithography can achieve higher resolution than optical, x-ray, or electron beam lithographic techniques because ions undergo no diffraction and scatter much less than electrons. In addition, resists are more sensitive to ions than to electrons. ***Figure 5.16*** depicts the computer trajectory of 50 H^+ ions implanted at 60 keV. As illustrated, the spread of the ion beam at a depth of 0.4 µm is only 0.1 µm. In addition, resists are more sensitive to ions than to electrons. There is also the possibility of a resistless wafer process. However, an ion beam is usually larger than an electron beam and the resolution is thus adversely affected. The most important application of ion lithography is the repair of masks for optical or x-ray lithography, a task for which commercial systems are available.

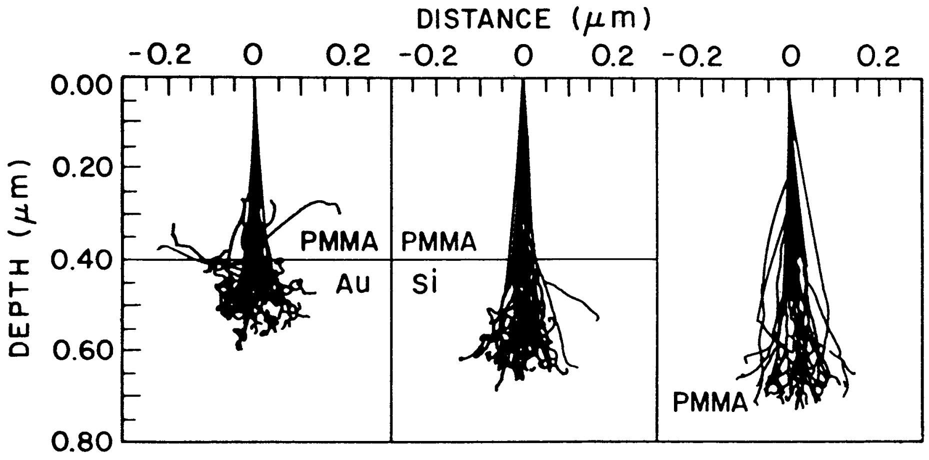

Figure 5.16: Trajectories of 60-keV H^+ ions traversing through PMMA into Au, Si, and PMMA.

5.9 Comparison of Lithographic Techniques

Optical lithography is the main stream technology and some commercially available resists can resolve down to 0.1 µm or lower. ***Figure 5.17*** shows the estimated resolution offered by the various lithographic techniques. The borderline of each technology is quite fuzzy. Generally speaking, optical lithography is considered difficult to use for a design rule of much less than 0.1 µm due to its resolution limit. For deep sub-micrometer structures, the two remaining options are electron beam direct writing or x-ray lithography. However, perfect x-ray masks are difficult to make and the throughput of electron lithography is slow (the throughput varies as the reciprocal of the square of the minimum feature length, that is, $\propto$ □l_m^{-2}). For mass production, the cost and footprint (required floor area) of the machine must also be minimized.

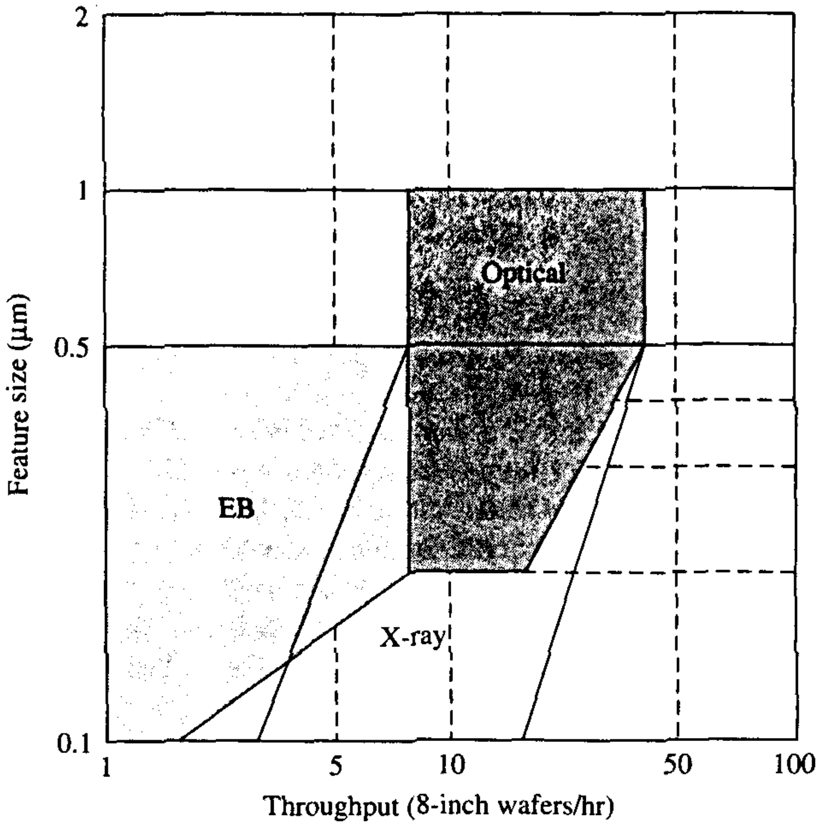

Figure 5.17: Resolution and throughput in the sub-micrometer region for opitcal, x-ray and electron-beam (EB) lithography.